AJAE

Open Access

Vol. 14, No. 1, pp. 14-27, March 2020
doi: https://doi.org/10.5572/ajae.2020.14.1.014
ISSN (Online) 2287-1160, ISSN (Print) 1976-6912

Research Article

Development and Field Application of a Passive Sampler for Atmospheric Mercury

Seung-Hwan Cha, Young-Ji Han*, Ji-Won Jeon†, Young-Hee Kim[1)], Hyuk Kim[1)], Seam Noh[1)], Myeong-Hee Kwon[1)]

Department of Environmental Science, Kangwon National University, Chuncheon, Gangwon-do 24341, Republic of Korea
[1)]Chemicals Research Division, National Institute of Environmental Research, Incheon 22689, Republic of Korea
†Current address: Center for Environmental Health and Welfare Research, Korea Institute of Science and Technology, 5 Hwarang-ro 14-gil, Seongbuk-gu, Seoul 02792, Republic of Korea

***Corresponding author.**
Tel: +82-33-250-8579
E-mail: youngji@kangwon.ac.kr

Received: 17 February 2020
Revised: 12 March 2020
Accepted: 16 March 2020

ABSTRACT In this study, a passive sampler for gaseous elemental mercury (GEM) was developed and applied to field monitoring. Three Radiello® diffusive bodies with iodine-impregnated activated carbon (I-IAC) as a Hg adsorbent were placed in an opaque acrylic external shield with a stainless steel lid. The performance of the passive sampler was evaluated at seven monitoring sites in South Korea. Hg uptake mass by the passive sampler linearly increased as the deployment time increased up to four months. The reproducibility of the sampler uptake mass for the different deployment periods was also good, and the average relative standard deviation calculated for the three adsorbents in one passive sampler was 9%. Using the Hg concentration measured by an active sampler, an experimental sampling rate (SR) of 0.082 m^3 day^{-1} was obtained. It was shown that the experimental SR was significantly affected by meteorological parameters, and a calibration equation was successfully derived based on wind speed, temperature, and relative humidity. With the calibrated SRs, there was a significant correlation between the active and passive Hg concentrations. When the passive samplers were deployed in an industrial district, the GEM concentration showed very large spatial variation, suggesting its potential for application in future field monitoring.

KEY WORDS Gaseous elemental mercury, Passive sampler, Iodine-activated carbon, Sampling rate, Calibration equation

1. INTRODUCTION

Mercury (Hg) has been categorized as a toxic substance by US Environmental Protection Agency (EPA). It exists as various compounds in environmental media, and methyl Hg, the most toxic form, readily accumulates in the food chain, causing potential adverse health effects in humans and wildlife (Wan *et al.*, 2009). Since Hg is the only heavy metal existing as a liquid under standard conditions, it can also exist as a gaseous form, resulting in active circulation between environmental media (Han *et al.*, 2004). The most common forms of atmospheric Hg are inorganic in nature, including gaseous elemental (GEM), gaseous oxidized (GOM), and particulate bound mercury (PBM). Due to its low reactivity and low dry and wet deposition velocities, GEM has a long residence time of 0.5–2 years (Gonzalez-Raymat *et al.*, 2017; Driscoll *et al.*, 2013; Lin and Peh-

konen, 1999), making it the predominant Hg form in the atmosphere. On the other hand, GOM, including $HgCl_2$, $HgBr_2$, HgO, $HgSO_4$, $Hg(NO_2)_2$, and $Hg(OH)_2$ (Gustin *et al.*, 2013; Hynes *et al.*, 2009), is considered to have high dry and wet deposition velocities, which results in a short atmospheric residence time of only a few days (Lin and Pehkonen, 1999). The sum of GEM and GOM is often referred to as total gaseous mercury (TGM).

According to the global mercury assessment by UNEP (2018), the atmospheric emission rate of Hg from anthropogenic sources in the United States and Europe is decreasing; although it continues to increase in Asia. In 2015, 49% of the 2,220 tons of global Hg emissions was emitted from Asia, with China contributing approximately 75% of Asia's total emissions (UNEP, 2018). Because Korea is situated in close proximity to China, the long-range transport of Hg from China is likely to be significant owing to predominantly westerly winds. There is also a need to assess the impact of recently applied regulatory policies on Hg emissions; therefore, it is necessary to develop an effective Hg monitoring system at the national level in Korea. Currently, there are 12 national monitoring sites for TGM in South Korea, with active samplers using cold vapor atomic fluorescence spectrometers. High temporal resolution of an active sampler is beneficial for identifying the possible sources and formation pathways, as well as tracking atmospheric conversion and transport mechanisms. However, an active sampler is expensive and requires electricity, a carrier gas, a relatively large space, and stringent management; therefore, it is difficult to operate at elevated mountain sites and/or very remote islands. On the other hand, passive samplers, having low manpower and easy management requirements, can be deployed at a fine spatial resolution (Vuong *et al.*, 2020; Carmichael *et al.*, 2003; Grosjean and Hisham, 1992), and have been widely used for persistent organic pollutants and carbon dioxide (Choi *et al.*, 2007; Harner *et al.*, 2004). Several studies have attempted to develop a passive sampler for atmospheric gaseous Hg (Zhang *et al.*, 2012; McLagan *et al.*, 2016a, b; Huang *et al.*, 2014), and various adsorbents such as gold (Brown *et al.*, 2012; Gustin *et al.*, 2011; Scott and Ottaway, 1981), silver (Gustin *et al.*, 2011), and sulfur-impregnated carbon (McLagan *et al.*, 2016b) have been used. Our group developed a passive sampler for GEM, consisting of three Radiello® diffusive bodies with gold-coated beads as the adsorbent installed in an acrylic external shield (Jeon *et al.*, 2019). Although there was a good relative standard deviation between three adsorbents, and the experimental sampling rate (SR) showed a good correlation with theoretical SR, the uptake rates were not correlated with the active Hg measurements in that previous study. In addition, the maximum deployment time was not sufficiently long, indicating that the sampler could not be applied for more than eight weeks, with an average gaseous Hg concentration of 2 ng m^{-3}. Some previous studies have also suggested a decrease in the uptake rate of gold with repeated use (McLagan *et al.*, 2016a; Huang *et al.*, 2012).

In this study, the adsorbent was changed to an iodine-impregnated activated carbon (I-IAC, Ohio Lumex Co., Cleveland, OH, USA)) in the same passive sampler design, and experimental evaluations of the sampler performance, including recovery tests and linearity tests, with deployment time were conducted. The developed I-IAC passive samplers were deployed at various locations to provide experimental SRs and for comparison with active Hg measurements. An empirical SR equation, calibrated with meteorological parameters, is also presented. The passive sampler was deployed in an industrial complex to determine the spatial variation of GEM concentrations.

2. EXPERIMENTS

2.1 Theory

A passive sampler uses a diffusion mechanism to collect pollutants, which can be explained by Fick's first law:

$$J = -D\frac{dC}{dx} = k \cdot dC = \frac{D}{L} \cdot dC \qquad \text{(Eq. 1)}$$

where J indicates the flux (mass · length^{-2} · time^{-1}), D (length^2 · time^{-1}) indicates the diffusion coefficient of a pollutant, and dC/dx (mass · length^{-4}) indicates the concentration gradient over a distance, x. In other words, the transported mass (flux J) is determined by the diffusivity of the pollutant (D), the diffusion layer length (L), and the concentration difference within a layer (dC). The diffusion layer length (L) and mass transfer coefficient (k) can be either theoretically or empirically estimated. The adsorption of a pollutant by laminar diffusion increases linearly with time, before gradually becoming curvilinear and ultimately no longer changing when an equilibrium is reached (McLag-

an *et al.*, 2016b; Bartkow *et al.*, 2005; Wania *et al.*, 2003). In order to accurately calculate the concentration using a passive sampler, it should be applied to the initial phase of this process, where the adsorption amount increases linearly.

Using a passive sampler, Hg concentration (ng m^{-3}) is calculated using the sorbed mass on the adsorbent (m in unit of ng), the deployment time of the passive sampler (t in unit of day), and the sampling rate (SR in unit of m^3 day^{-1}) (Eq. 2); therefore, it is critical to use an accurate SR.

$$\text{Conc.} = \frac{m}{t \cdot SR} \quad \text{(Eq. 2)}$$

SR can be theoretically calculated by the product of the mass transfer coefficient (k in Eq. 1) and the area over which diffusion occurs. However, many studies have provided experimental SRs instead of using theoretical SRs when developing a passive sampler because (i) it is difficult to estimate a diffusive layer thickness and (ii) turbulence (as well as laminar diffusion) affects the adsorption in practical application (Jeon *et al.*, 2019; McLagan *et al.*, 2018; Guo *et al.*, 2014; Peterson *et al.*, 2012). To develop an experimental SR, the uptake amount (m) of a passive sampler should be compared with the concentration measured by a reliable active sampler (C_{act}) (Eq. 3).

$$\text{SR} = \frac{m}{t \cdot C_{act}} \quad \text{(Eq. 3)}$$

2.2 Sampler Preparation

The passive sampler consisted of an adsorbent, diffusive body, and external shield. I-IAC was used as the adsorbent and Radiello® (Sigma-Aldrich) having a 25-μm pore size was used as the diffusive body. Inside a HDPE opaque acrylic body, three Radiello® bodies containing 0.50 ± 0.025 g of I-IAC were connected to the top of the inside of the external shield. To protect the sampler from small insects, rain, wind, and dust, the bottom of the external shield was covered with stainless steel. A detailed description of the passive sampler design can be found in our previous study (Jeon *et al.*, 2019). There is unpublished data showing that GOM rarely passes through the Radiello diffusive body (Stupple *et al.*, 2019); therefore, Hg collected by the passive sampler was regarded as GEM in this study. Before sampling, I-IAC was heated at 150°C for 4 h to remove any residual Hg. The Radiello® was cleaned with detergent and ultrapure water using an ultrasonic bath, dried on a clean bench, and triple sealed in zipper bags until usage. After being cleaned with detergent and ultrapure water, the external shield was soaked in a 1% HCl solution at 60°C for 36 h and dried on a clean bench.

To identify the adsorption efficiency of the I-IAC, a recovery test was conducted by injecting different volumes of Hg^0-saturated vapor (using mercury ≥99.99%, trace metal basis, Sigma-Aldrich) into a closed 40-mL glass vial containing the same amount of I-IAC (0.5 g) as was used in the passive sampler. After injecting Hg^0-saturated vapor using a gas-tight syringe (Microliter™#725, HAMILTON CO., Reno, NV, USA), the vials were left on a clean bench for 7 days to facilitate adsorption before the analysis. The injected amounts were 3.2, 6.4, 9.6, 12.9, and 16.1 ng of Hg^0.

2.3 Outdoor Sampling for Performance Evaluation

The passive sampler was deployed on the roof of a four-story building at Kangwon National University, Chuncheon, Korea for evaluation purposes. From Aug. 3, 2018 to Jan. 1, 2019, seven sets of passive samplers were deployed with different mounting periods from 24 to 92 days (Table 1). In addition, eight sets of passive samplers were initially deployed simultaneously on May 1, 2019, with one sampler randomly retrieved every week or every month and analyzed to measure the Hg uptake amount from week 1 to week 17 (Table 1). During the second period of sampling in 2019, atmospheric TGM concentrations were simultaneously measured using an active sampler (Tekran 2537X., Toronto, Canada), which is the most widely used type of active sampler (Jeon *et al.*, 2019; Slemr *et al.*, 2003). The Tekran 2537X includes two gold traps alternately

Table 1. Summarization of the outdoor sampling for performance evaluation.

Location	Deployment time	Period	No. of sets
Chuncheon	24~92 days	2018.08.03~2019.01.01	7
	7~119 days	2019.05.01~2019.08.28	8
Imsil	27~56 days	2018.06.22~2018.12.17	9
	14~28 days	2019.06.13~2019.07.11	3
Bulgwang	27~56 days	2018.06.22~2018.12.06	9
Ulsan	28~56 days	2018.06.25~2018.12.11	4
Deokjeok Island	28~56 days	2018.06.25~2018.11.12	7
Taean	13~28 days	2019.05.15~2019.06.12	3
Gwangyang	13~41 days	2019.07.11~2019.08.21	3

collecting and thermally desorbing Hg every 5 min; it then quantifies TGM using a cold vapor atomic fluorescence spectrometer (CVAFS). Auto-calibration was performed using an internal permeating source every 24 h. Although the Hg species that the Tekran 2537X measured was TGM, many studies have shown that most of the TGM exists as GEM in ambient air (> 97%) in Korea, as well as in other areas (Jeon *et al.*, 2019; Lee *et al.*, 2016; Han *et al.*, 2014; Valente *et al.*, 2007; Aspmo *et al.*, 2006; Poissant *et al.*, 2005; Gabriel *et al.*, 2005; Schroeder and Munthe, 1998; Slemr *et al.*, 1985); hence, the experimental sampling rate was calculated using the Tekran TGM data in Eq. 3. Reproducibility was calculated from the three Radiello bodies with I-IAC contained in one sampler.

In addition to Chuncheon, 38 sets of the passive samplers were deployed at six different sites in South Korea during the years 2018 and 2019 to identify the spatial variation in GEM uptake (Table 1, Fig. 1). The Tekran 2537X samplers were deployed at the same locations in 2019 to determine the experimental SR and to compare between the passive and active concentrations. An automatic weather station (Vintage Pro2, DAVIS Instruments, Hayward, CA, USA) was also installed at the sampling locations to obtain meteorological data, including temperature, humidity, wind speed, and wind direction at sites in Chuncheon, Imsil, Taean, and Gwangyang in 2019. However, it was not possible to obtain both meteorological data and Tekran TGM measurements at the sampling locations in 2018.

2.4 Field Application to Industrial District

The passive samplers were deployed in the Onsan national industrial district in Ulsan where zinc smelters, chemical plants, and a hazardous waste landfill site are located. According to a previous study in which the air-soil Hg exchange flux in the landfill area in this industrial district was measured (Kim *et al.*, 2013), atmospheric Hg concentrations were anticipated to be very high. Seventeen sets of passive samplers were placed at intervals of about 1 km (Fig. 1). Since the Hg concentrations were anticipated to be very high in this area, the passive samplers were deployed for only four days, from Aug. 22 to 26, 2019. Among the industries located in the Onsan national district, the zinc smelters are considered to be the largest Hg emitters (Fig. 1). Meteorological data were obtained at the BM1 and M2 sites. The BM1, B2, and B3 sites were regarded as background sites.

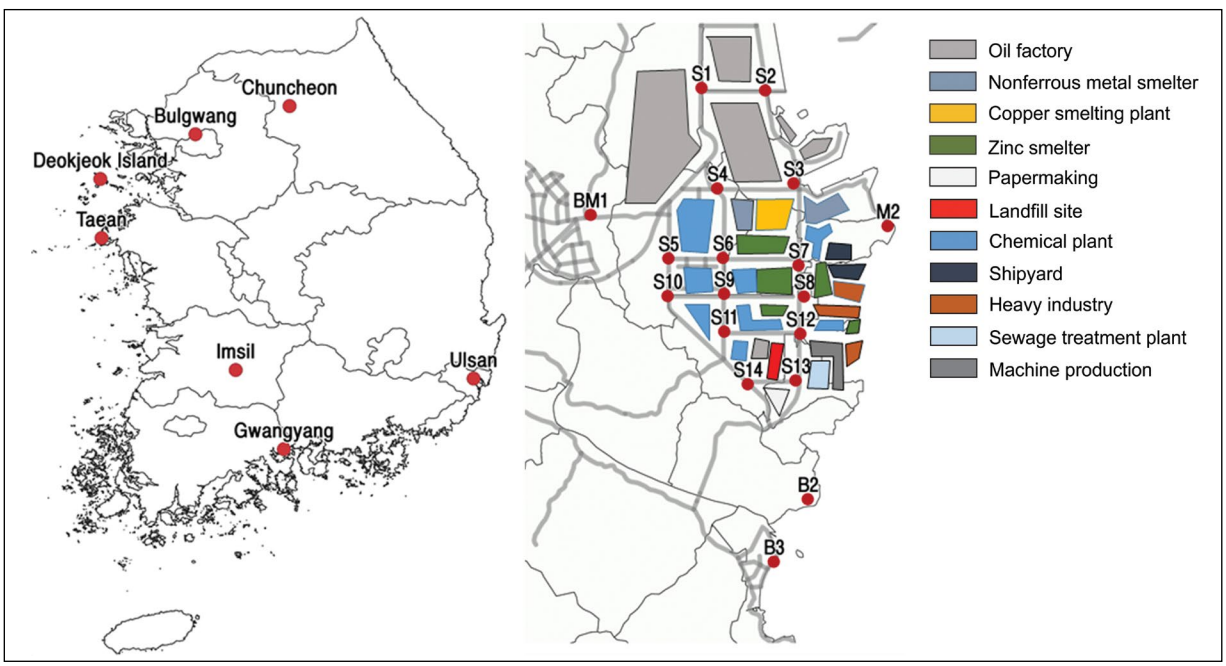

Fig. 1. The sampling sites for the performance evaluation in South Korea (left) and in the Onsan national industrial district in Ulsan (right). Note that the meteorological data were obtained from BM1 and M2.

2.5 Analysis

The I-IAC adsorbents were analyzed using a cold vapor atomic absorption spectrometer (DMA-80, Milestone, Italy). Before the analysis, an empty boat was heated to remove all residual Hg and a Hg standard solution (SRM 3133, NIST) was used to produce a calibration curve (r^2 should be greater than 0.99). A standard reference material (SRM, MESS-3, marine sediment reference material) was analyzed every six samples to check the analytical precision, and the relative standard deviation was 6.3%. Each I-IAC adsorbent was then analyzed at least three times in about 0.02–0.1 g aliquots, and the average RSD was 7.8 ± 3.9%. Field blanks were treated in the same manner as the samples, including air exposure during sampler deployment and retrieval. The average Hg mass of the field blanks was 0.18 ± 0.22 ng · g^{-1}-IAC (n = 12), which was much lower than that in the samples. All data shown in the following sections were field blank corrected.

3. RESULTS AND DISCUSSION

3.1 Blank and Recovery Test

When 0.5 g of I-IAC, the same amount used in the passive sampler, was analyzed without any treatment, the Hg mass was 1.0–1.2 ng. When I-IAC was pre-heated at 150°C for 4 h, the blank value was less than the analytical detection limit. The recovery rate, identified by injecting different volumes of Hg^0-saturated vapor into a vial containing 0.5 g of I-IAC, ranged from 72 to 147% (Fig. 2). The r^2 value for the correlation between the injection amount and the recovered amount was 0.95, but the slope was only 0.76 because the recovery rate somewhat decreased as the injection amount increased (Fig. 2). A low recovery rate at a high injection amount was possibly a result of the injection amount exceeding the I-IAC adsorption capacity of 0.5 g. However, the linearity between the injection amounts and the recovery rates was good and consistent, and there was no critical point at which the recovery rate dropped dramatically (Fig. 2); therefore, it was unlikely a result of breakthrough from the I-IAC. The adsorption capacity of the I-IAC was also tested in the field (results shown in following section). The lower recovery rate at the higher injection amount was possibly derived from either (i) an increase in Hg adsorption onto the surface of the glass vial or (ii) insufficient time for Hg adsorption onto the I-IAC. Further study is required to accurately determine the recovery rate and the adsorption efficiency of I-IAC; Teflon, rather than glass, vials should be used to prevent Hg adsorption and to allow sufficient time for an Hg-adsorption equilibrium to develop between I-IAC and air in the vial.

3.2 Linearity with Deployment Time

In order to evaluate performance, a passive sampler was deployed for 63 days from Aug. 3 to Jan. 1, 2019 and for about four months from May 1 to Aug. 28, 2019 in Chuncheon. Using all data obtained over two years, the Hg uptake mass was seen to linearly increase as deployment time increased, and the coefficient of determination (r^2) and the slope were 0.935 and 0.16 (ng day^{-1}), respectively (Fig. 3). When the y-intercept was forced through zero, the slope slightly increased to 0.17. The TGM concentration measured by the active sampler (Tekran 2537X, cold vapor atomic fluorescence spec-

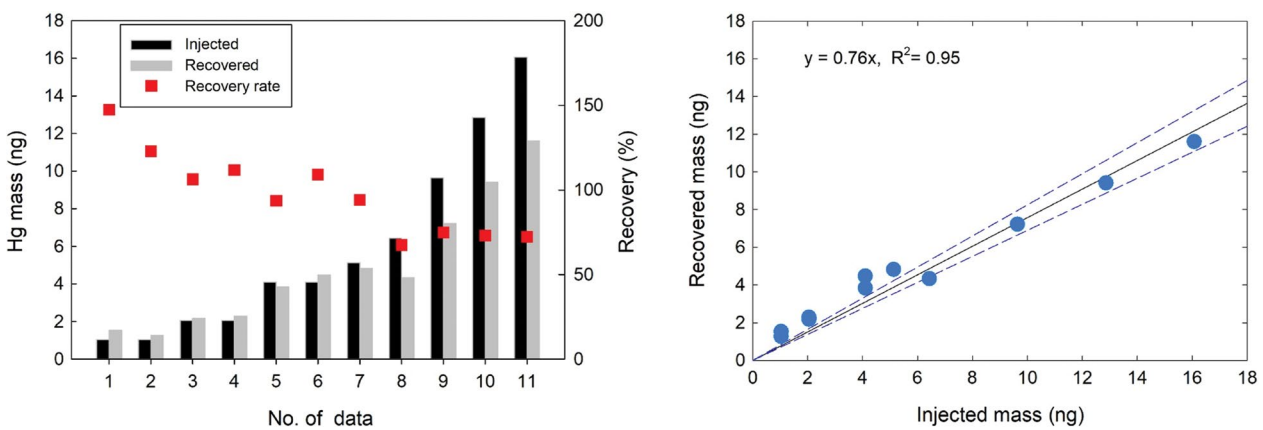

Fig. 2. Recovered Hg mass with each injected mass (left), and the linear regression between injected and recovered mass (right). The red rectangular points indicate the recovery rates in the left panel.

trometry) during 2019 was relatively consistent, ranging from 2.1 to 2.5 ng m^{-3} (average = 2.3 ng m^{-3}) throughout the sampling period. The linearity shown in Fig. 3 indicates that the uptake capacity of the passive sampler was likely to be more than four months (equal to 21.7 ng of Hg uptake mass), with a typical atmospheric Hg concentration of about 2 ng m^{-3}. Compared with a previous study using gold-coated beads as an adsorbent at the same location (Chuncheon), the uptake rates were similar between the gold beads and I-IAC at similar TGM concentrations (Jeon *et al.*, 2019), showing that both adsorbents provided an effective adsorptive surface for GEM in the passive sampler. However, the amount of Hg adsorbed per mass of adsorbent was about two times higher for the I-IAC (0.32 ng-Hg · g^{-1}-IAC) than for the gold beads (0.17 ng · g^{-1}-gold). In addition, Hg uptake mass increased linearly up to four months in this study, whereas it increased only up to eight weeks when using the gold-coated beads (Jeon *et al.*, 2019), indicating that the maximum adsorption capacity of the I-IAC was much higher than that of the gold-beads.

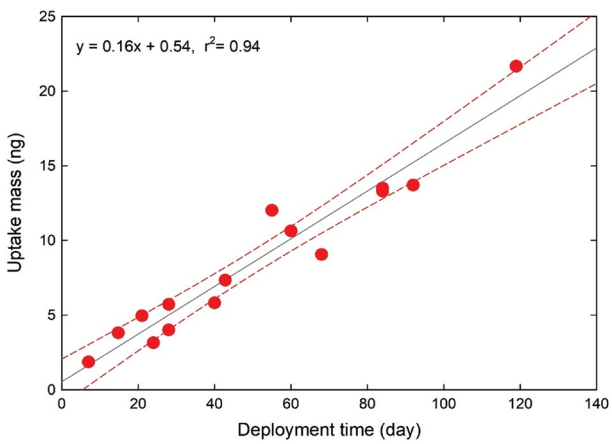

Fig. 3. Increase of Hg uptake mass with the increase of deployment time at the Chuncheon site. The red dash lines indicate the 95% of confidence intervals for the regression.

The samplers were also deployed at seven different sites in 2018 and 2019 (Table 1) to determine the spatial variation of the uptake rate and to evaluate the reproducibility over different deployment periods. Two samplers were deployed at each site for one month each (or for 2 weeks each in Taean) and one other sampler was deployed for two consecutive months (or for two consecutive 2-week periods in Taean). The two uptake masses were compared. If the sum of the adsorption amounts of the two samplers deployed for one month each (or for 2 weeks each) was the same as the adsorption amount of the sampler deployed for two consecutive months (or for two consecutive 2-weeks), the uptake mass was considered to have increased linearly with deployment time. In Fig. 4, the orange and the blue bars represent the Hg uptake mass of the passive sampler deployed for one month each (or for 2 weeks each), and the grey bar represents the Hg mass for two consecutive months (or for two consecutive 2-week periods). Among the 13 sets, two sets showed quite large differences between the two Hg amounts (one each in Bulkwang and Ulsan), and all other sets showed similar uptake masses. The average relative difference was 14%; however, this was 9% when the two sets having large variation were excluded. These results indicate that the Hg adsorption amount increased linearly for about two months and that the reproducibili-

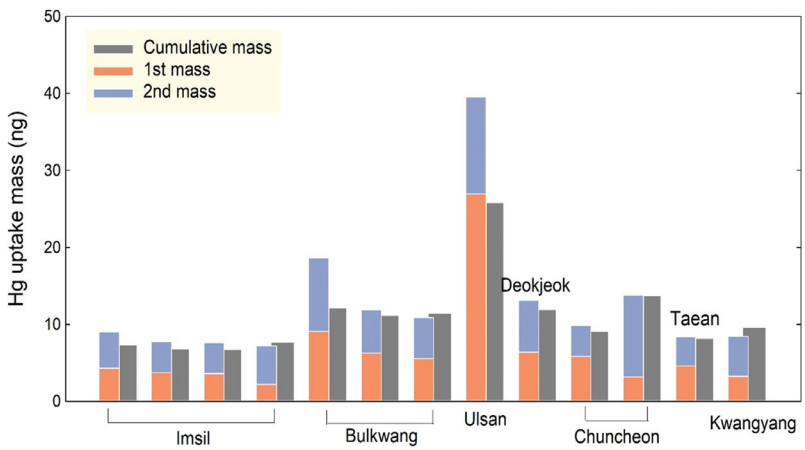

Fig. 4. Reproducibility of the passive sampler for different deployment periods.

ty of the sampler uptake amount for the different deployment periods was also good. In Chuncheon, the sampler was also deployed for three consecutive months and compared with three samplers deployed for one month each. Here, the uptake mass for the three consecutive months (13.7 ng) was almost identical to the sum of the uptake amounts of the three one-month samplers (13.0 ng).

The sampler consists of three diffusive bodies containing I-IAC. Therefore, the relative standard deviation (RSD) can be calculated for the three uptake masses; the average and median RSD were 9.0% and 6.5%, respectively. Some previous studies have shown good RSD results from collocated Hg passive samplers. McLagan *et al.* (2018) and Zhang *et al.* (2012) presented RSD values of 4% and 12%, respectively, for replicates from samplers using sulfur-impregnated activated carbon. Skov *et al.* (2007) used gold-beads as the adsorbent in their Hg passive sampler, reporting an RSD value of 7.7%. In study, the overall precision from two collocated samplers was not evaluated, and an evaluation of the relevant QA/QC is required.

3.3 Uptake Rate

Uptake rate (ng day^{-1}) is calculated by uptake mass divided by deployment time. The uptake rate significantly varied among the sites, ranging from 0.21 ng day^{-1} at the Chuncheon site to 0.30 ng day^{-1} at the Taean site. When the uptake rates were compared with the TGM concentrations measured by the Tekran 2537X at each site, they tended to follow the TGM concentration relatively well, despite small differences in TGM concentration (Fig. 5). The correlations between uptake rate and TGM concentration were good at the Imsil, Taean, and Gwangyang sites, whereas the r^2 value was only about 0.48 at the Chuncheon site. At the Chuncheon site, the white point in Fig. 5, which did not well reflect the TGM concentration, represents the uptake rate of the passive sampler deployed only for 1 week. There is a possibility that one-week deployment was not sufficiently long to infer the atmospheric Hg concentration; in future, it is necessary to study the minimum required deployment period of the passive sampler. Although the correlations between the uptake rates of the passive sampler and the TGM concentrations were relatively good at each site, such a tendency was not observed when plotting all data from all sites, probably because the SR varied under different meteorological conditions (McLagan *et al.*, 2017; Huang *et al.*, 2014).

3.4 Sampling Rate

The SR is required to calculate concentration when

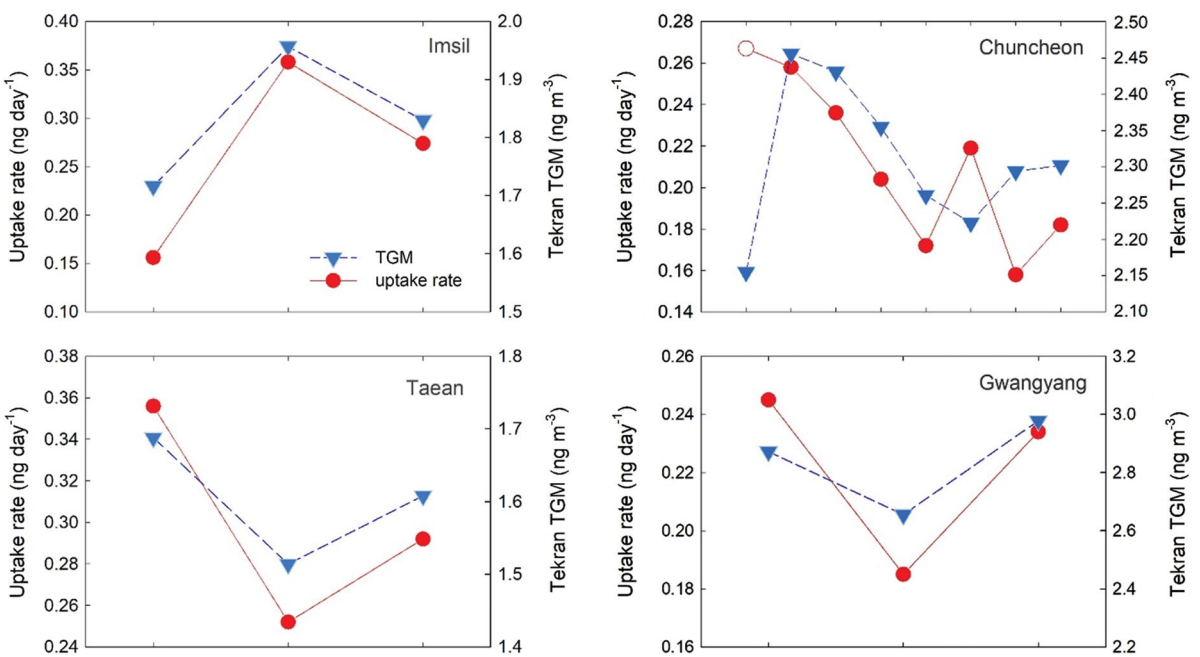

Fig. 5. Correlation between Tekran TGM concentration and the uptake rate of the passive sampler at each site. The white point observed in the graph for Chuncheon (the upper right graph) indicates the uptake rate of the passive sampler deployed for 1 week.

using a passive sampler. Although SR can be theoretically calculated using Eq. 3, it is difficult to estimate the diffusive lengths, which are affected by sampler design (McLagan *et al.*, 2016b; Armitage *et al.*, 2013; Fuller *et al.*, 1966). In addition, a passive sampler is intentionally or unintentionally dependent on meteorological parameters (Jeon *et al.*, 2019; McLagan *et al.*, 2017; Skov *et al.*, 2007). Therefore, many studies have provided experimental SRs using the concentrations measured by an active sampler (Jeon *et al.*, 2019; McLagan *et al.*, 2018; Guo *et al.*, 2014; Peterson *et al.*, 2012). Average SRs were 0.14 ± 0.05, 0.09 ± 0.02, 0.18 ± 002, and 0.08 ± 0.01 m^3 day^{-1} at the Imsil, Chuncheon, Taean, and Gwangyang sites, respectively, resulting in an overall average of 0.114 ± 0.05 m^3 day^{-1} across all data (Fig. 6).

McLagan *et al.* (2018) provided an experimental SR using linear regression, as shown in Eq. 3. When a linear regression using the uptake mass (m), Tekran TGM concentration (C_a), and deployment time of the passive sampler (t) was performed, the slope (which is the SR) was 0.082 m^3 day^{-1}, and the correlation between two variables was very good (Pearson r = 0.92) (Fig. 6). Compared with the SR (0.135 ± 0.003 m^3 day^{-1}) suggested by McLagan *et al.* (2018) using a similar passive sampler design, the SRs observed in the present study are relatively low. Although there was a significant regression between $C_a \times t$ and m, as shown in Fig. 6, the SR varied significantly among the samples across all sites because the uptake mass of the passive sampler was susceptible not only to the concentration of pollutant but also to parameters such as temperature and wind speed (McLagan *et al.*, 2017; Guo *et al.*, 2014).

To evaluate the effects of meteorological factors, the relationship between SR and meteorological variables was identified. During the sampling period, air temperature ranged from 16.9°C to 28.6°C, wind speed (WS) ranged from 0.5 to 3.2 m s^{-1}, and relative humidity (RH) ranged from 42.6 to 81.8%. The experimental SRs showed a negative relationship with temperature (p-value = 0.02, Pearson r = −0.557), but there was no statistically significant correlation with RH or WS. The negative correlation with temperature was not anticipated because diffusion coefficient theoretically increases as temperature increases, hence increasing SR. Also, there have been some previous studies suggesting that SR was positively affected by WS (Jeon *et al.*, 2019; McLagan *et al.*, 2018, 2017), indicating that turbulence affected mass transport from the atmosphere to the adsorbent. In this study, it was also observed that the SR decreased with an increase in TGM concentration. TGM concentration also increased with temperature increase, possibly because GEM was emitted from the soil and/or water surfaces under intense sunlight and high temperature (Park *et al.*, 2014; Poissant *et al.*, 2000); this positive correlation between temperature and TGM concentration possibly caused the negative relationship between SR and TGM concentration. Whether a decrease in SR was caused directly by an increase in TGM concentration or indirectly by the interrelationship between TGM concentration and temperature was not clear. Because of the non-linear interactions between uptake rate and other parameters, it is difficult to derive the calibration equation of the SR.

In order to calibrate SR with the meteorological factors, a multi-linear regression was performed after all variables were normalized by the averages. We found a

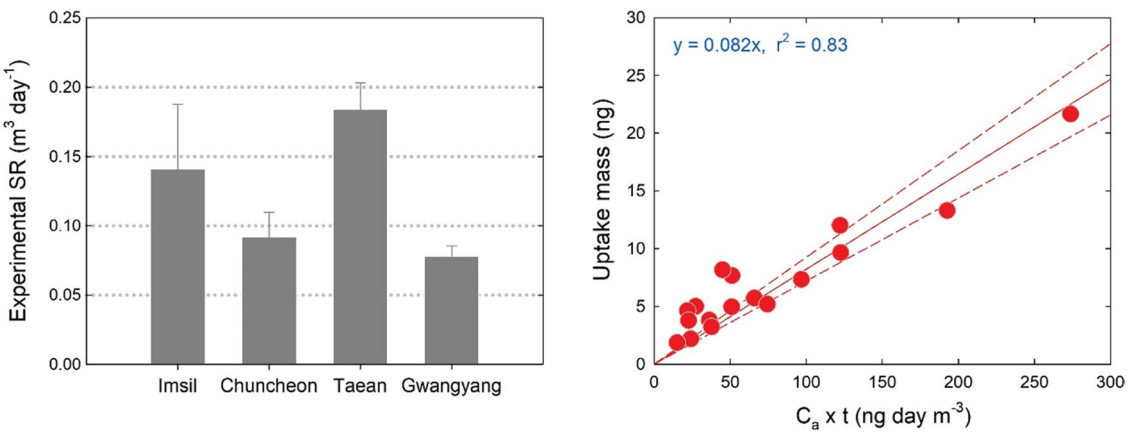

Fig. 6. The experimental SRs at each sampling location (left) and a SR obtained from a linear regression (right).

statistically significant multiple linear relationship between SR, temperature, and RH:

$$SR(m^3\ day^{-1}) = -(0.209 \pm 0.044)\ T_a/T_{avg} + (0.146 \pm 0.037)\ RH/RH_{avg} + (0.177 \pm 0.048),\ r^2 = 0.68 \quad \text{(Eq. 4)}$$

The multiple linear equation fits the data well (p-value < 0.001) and both variables of T_a (p-value < 0.001) and RH (p-value $= 0.001$) and the constant (p-value $= 0.003$) were statistically significant. When WS exceeded or was equal to 1.0 m s^{-1}, it was included as a significant positive variable for SR, giving the following equation:

$$SR(m^3\ day^{-1}) = -(0.214 \pm 0.023)\ T_a/T_{avg} + (0.038 \pm 0.011)\ WS/WS_{avg} + (0.077 \pm 0.027)\ RH/RH_{avg} + (0.204 \pm 0.026),\ r^2 = 0.92 \quad \text{(Eq. 5)}$$

All variables were statistically significant (p-values were < 0.001, 0.006, 0.018, and < 0.001 for T_a, WS, RH, and the constant, respectively). The better fit of Eq. 5 than that of Eq. 4 suggests that the effect of WS on SR was not consistent, and only wind speed above a certain level (1 m s^{-1} in this study) positively affected the SR, probably due to a turbulence effect.

3.5 Comparison with Active Sampler

Many previous studies have used a constant SR to convert uptake mass to a concentration unit (Gouin *et al.*, 2005a; Pozo *et al.*, 2004; Shoeib and Harner, 2002). However, SR is in fact affected by meteorological parameters such as WS, sampler design, and even the mounting height of the sampler (Huang *et al.*, 2014; Gustin *et al.*, 2011; Fan *et al.*, 2006); therefore, it is necessary to infer the concentration using a calibrated SR. When using a constant SR, i.e., 0.082 $m^3\ day^{-1}$ from Fig. 6, there was no correlation between the Tekran TGM concentration and the passive Hg concentration (left panel of Fig. 7). However, the concentrations obtained using the calibrated SR (from Eqs. 4 and 5) were significantly correlated with the Tekran TGM concentration, and most data points converged on the 1:1 line (Fig. 7). The average relative difference between the passive and active (Tekran 2537X) concentrations was 31% and 15% when using the constant SR and calibrated SRs, respectively. The two graphs in Fig. 7 strongly suggest that the calibrated SR should be used when calculating concentrations using the passive sampler developed in this study. Fig. 7 was obtained from the data collected from four different sites, indicating that one calibration equation for SR can provide a reliable Hg concentration, even at different locations.

3.6 Spatial GEM Distribution in the Industrial District

In order to identify the spatial GEM concentration in a large Hg emission area, the passive samplers were deployed in the Onsan industrial district (Fig. 1). Since it was shown that the SR was significantly affected by meteorological parameters, the GEM concentrations were calculated using the SRs calibrated by Eq. 4 when WS was less than 1 m s^{-1} and by Eq. 5 when WS exceeded 1 m s^{-1}. The meteorological data were obtained from

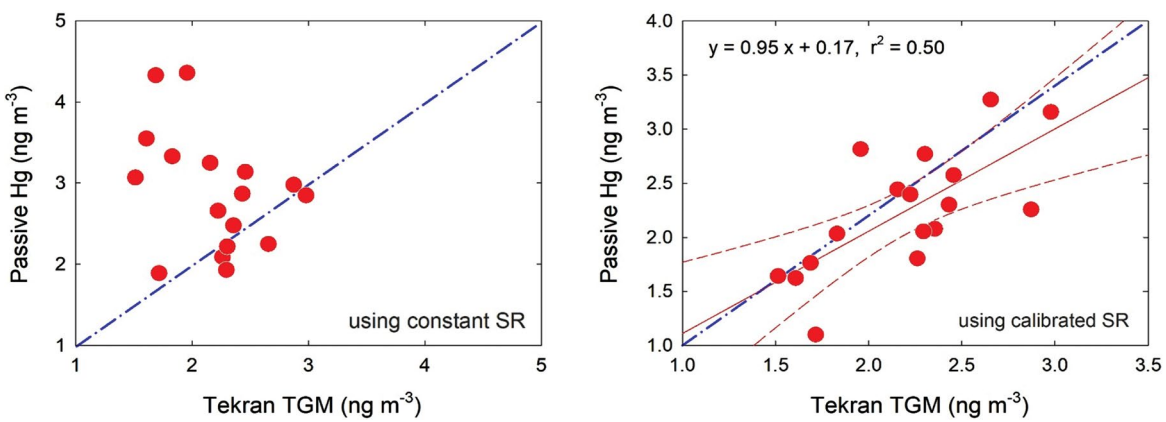

Fig. 7. Comparison between the passive and the active Hg concentration using a constant SR (left) and the calibrated SRs (right). The blue dash line indicates the 1:1 line, and the red dash lines represent the 95% of confidence interval for the regression.

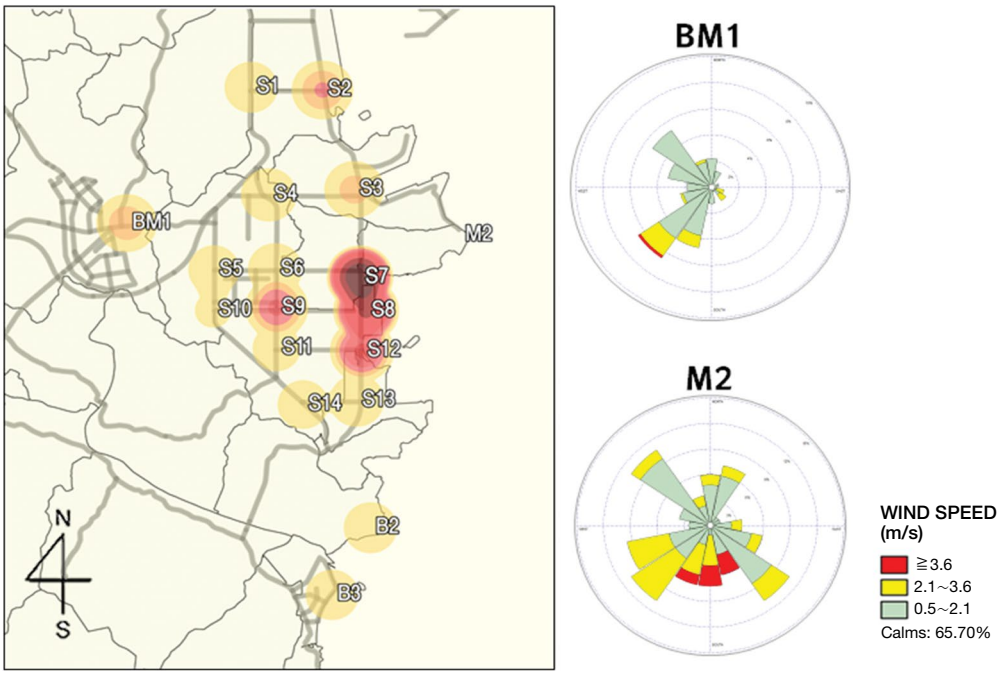

Fig. 8. Spatial variation of the GEM concentration measured by the passive sampler and the wind rose plots in the Onsan national industrial complex.

two locations, BM1 and M2 (Fig. 1), and the WS showed a large difference at the two locations (average WS was 0.58 m s^{-1} and 1.77 m s^{-1} at BM1 and M2, respectively), whereas temperature and relative humidity were not significantly different between the two sites. The meteorological parameters obtained for the M2 site located by the East Sea were applied to calibrate the SRs for the sites B2, B3, S3, S7, S8, S11, S13, and S14, and those obtained from the BM1 site were used to calibrate the SRs for the sites BM1, S4, S5, S6, S9, and S10. The calibrated SRs averaged 0.110 m^3 day^{-1} and 0.143 m^3 day^{-1} for BM1 and M2, respectively.

The GEM concentrations showed a very large spatial variation in the industrial district, ranging from 0.6 to 118.8 ng m^{-3} (average = 14.5 ng m^{-3}). The highest GEM concentrations were observed at the S7 and S8 sites near the largest zinc smelter in Korea. According to the national report for the Hg content of hazardous wastes (Park *et al.*, 2010), zinc smelters show the highest Hg content among waste sludge. The GEM concentration was also high at S12 (21.9 ng m^{-3}), which was located northeast of a large hazardous waste landfill and near the zinc smelter. On the other hand, the GEM concentrations were relatively low at the background sites B2 (1.9 ng m^{-3}) and B3 (1.8 ng m^{-3}).

4. CONCLUSION

In this study, a passive sampler for GEM was developed and applied in field monitoring. Based on the sampler design used in a previous study (Jeon *et al.*, 2019), the adsorbent was changed from gold-coated beads to I-IAC. In order to evaluate performance, the passive samplers were initially deployed and one sampler was randomly retrieved every week or every month. Hg uptake amount linearly increased up to four months. Compared with a previous study using gold-coated beads as the adsorbent at the same location, the uptake rates were similar for gold beads and I-IAC under similar atmospheric Hg concentrations. However, the amount of Hg adsorbed per mass of I-IAC was about two times higher than that of the gold-beads. When the samplers were deployed at seven monitoring sites, the reproducibility of the sampler uptake amount for the different deployment periods was also good.

The uptake rates varied significantly among the sites, ranging from 0.21 ng day^{-1} to 0.30 ng day^{-1}. There were good correlations between the uptake rates of the passive sampler and the Hg concentrations of the active sampler at each site. However, when the data obtained from all sites were plotted together, no relationship between

uptake rate and Hg concentration was seen. There was a significant linear regression between the product of the Hg uptake mass of the passive sampler and the deployment time and Hg concentration of the active sampler; a slope (representing the SR) of 0.082 m^3 day^{-1} was obtained. However, the experimental SRs obtained at various sampling locations showed large variation owing to the effects of meteorology. In this study, SR was positively correlated with RH and WS (only when WS exceeded 1 m s^{-1}) and negatively correlated with temperature. This unexpected negative relationship between temperature and SR was possibly caused by the interacting effects of additional parameters. In future, in order to prevent such influences, only one variable should be adjusted while the others are held constant in lab experiments. A calibration equation for SR was presented, using the variables WS, temperature, and RH ($r^2 = 0.92$ between the experimental SRs and the calibrated SRs). When the passive and active Hg concentrations were compared, there was no correlation when using a constant experimental SR; however, the passive GEM concentrations were significantly correlated with the active Hg concentrations when using the calibrated SRs; the percent difference was 15%. In order to identify the spatial variation in GEM concentration in a large Hg emission region, the passive samplers were deployed at a fine spatial resolution in the national industrial district. The GEM concentration varied significantly and the highest concentrations appeared near a large zinc smelter.

This study has some limitations. Although a calibration equation for SR was derived, the data were obtained only from a field application; a lab study with precise control of affecting parameters was not performed. Therefore, the calibration equation can be only used within the ranges of the observed meteorological conditions prevalent in this study. In addition, the maximum deployment time for the passive sampler should be investigated since the outdoor experiments were conducted only up to four months in this study. However, the good correlation between the uptake rates of the passive sampler and the Hg concentrations at each sampling site suggest a possible application in future field monitoring studies.

ACKNOWLEDGEMENT

This work was funded by a National Institute of Environmental Research (NIER-SP2017-112) and by a National Research Foundation of Korea (NRF) grant funded by the Korean government (MSIP) (Grant No. 2019R1F1A1062742).

REFERENCES

Armitage, J.M., Hayward, S.J., Wania, F. (2013) Modeling the uptake of neutral organic chemicals on XAD passive air samplers under variable temperatures, external wind speeds and ambient air concentrations (PAS-SIM). Environmental Science & Technology, 47, 13546–13554, https://doi.org/10.1021/es402978a.

Aspmo, K., Temme, C., Berg, T., Ferrari, C., Gauchard, P., Fain, X., Wibetoe, G. (2006) Mercury in the atmosphere, snow and melt water ponds in the north atlantic ocean during arctic summer. Environmental Science & Technology, 40(13), 4083–4089, https://doi.org/10.1021/es052117z.

Bartkow, M.E., Booij, K., Kennedy, K.E., Muller, J.F., Hawker, D.W. (2005) Passive air sampling theory for semivolatile organic compounds. Chemosphere, 60, 170–176, https://doi.org/10.1016/j.chemosphere.2004.12.033.

Brown, R.J.C., Burdon, M.K., Brown, A.S., Kim, K.-H. (2012) Assessment of pumped mercury vapouradsorption tubes as passive samplers using a micro-exposure chamber. Journal of Environmental Monitoring, 14, 2456–2463, https://doi.org/10.1039/c2em30101f.

Carmichael, G.R., Ferm, M., Thongboonchoo, N., Woo, J.H., Chan, L.Y., Murano, K., Viet, P.H., Mossberg, C., Bala, R., Boonjawat, J., Upatum, P., Mohan, M., Adhikary, S.P., Shrestha, A.B., Pienaar, J.J., Brunke, E.B., Chen, T., Jie, T., Guoan, D., Peng, L.C., Dhiharto, S., Harjanto, H., Jose, A.M., Kimani, W., Kirouane, A., Lacaux, J., Richard, S., Barturen, O., Cerda, J.C., Athayde, A., Tavares, T., Cotrina, J.S., Bilici, E. (2003) Measurements of Sulfur Dioxide, Ozone and Ammonia Concentrations in Asia, Africa, and South America Using Passive Samplers. Atmospheric Environment, 37(9–10), 1293–1308, https://doi.org/10.1016/s1352-2310(02)01009-9.

Chapman, S., Cowling, T.G. (1939) The mathematical theory of non-uniform gases, 3rd ed. The Mathematical Gazette, 257, 488, https://doi.org/10.2307/3607024.

Choi, S.-D., Baek, S.-Y., Chang, Y.-S. (2007) Influence of a large steel complex on the spatial distribution of volatile polycyclic aromatic hydrocarbons (PAHs) determined by passive air sampling using membrane-enclosed copolymer (MECOP). Atmospheric Environment, 41, 6255–6264, https://doi.org/10.1016/j.atmosenv.2007.03.058.

Driscoll, C.T., Mason, R.P., Chan, H.M., Jacob, D.J., Pirrone, N. (2013) Mercury as a global pollutant: Sources, pathways and effects. Environmental Science & Technology, 47, 4967–4983, https://doi.org/10.1021/es305071v.

Fuller, E.N., Schettler, P.D., Giddings, J.C. (1966) New method for prediction of binary gas-phase diffusion coefficients. Industrial & Engineering Chemistry, 58, 18–27, https://

doi.org/10.1021/ie50677a007.

Gabriel, M.C., Williamson, D.G., Brooks, S., Lindberg, S. (2005) Atmospheric speciation of mercury in two contrasting southeastern US airsheds. Atmospheric Environment, 39(27), 4947–4958, https://doi.org/10.1016/j.atmosenv.2005.05.003.

Gan, S.-Y., Yi, S.-Y., Han, Y.-J. (2009) Characteristics of atmospheric speciated gaseous mercury in Chuncheon, Korea. Journal of Korean Society of Environmental Engineers, 31, 382–391,

Gonzalez-Raymat, H., Liu, G., Liriano, C., Li, Y., Yin, Y., Shi, J. (2017) Elemental mercury: Its unique properties affect its behavior and fate in the environment. Environmental Pollution, 229, 69–86, https://doi.org/10.1016/j.envpol.2017.04.101.

Gouin, T., Harner, T., Blanchard, P., Mackay, D. (2005) Passive and active air samplers as complementary methods for investigating persistent organic pollutants in the Great Lakes basin. Environmental Science & Technology, 39, 9115–9122, https://doi.org/10.1021/es051397f.

Grosjean, D., Williams II, E.L. (1992) A Passive Sampler for Atmospheric Ozone. Journal of the Air & Waste Management Association, 42(2), 169–173, https://doi.org/10.1080/10473289.1992.10466980.

Guo, H., Lin, H., Zhang, W., Deng, C., Wang, H., Zhang, Q., Shen, Y., Wang, X. (2014) Influence of meteolorogical factors on the atmospheric mercury measurement by a novel passive sampler. Atmospheric Environment, 97, 310–315, https://doi.org/10.1016/j.atmosenv.2014.08.028.

Gustin, M.S., Huang, J., Miller, M.B., Peterson, C., Jaffe, D.A., Ambrose, J., Finley, B.D., Lyman, S.N., Call, K., Talbot, R., Feddersen, D., Mao, H., Lindberg, S.E. (2013) Do We Understand What the Mercury Speciation Instruments Are Actually Measuring? Results of RAMIX. Environmental Science & Technology, 47, 7295–7306, https://doi.org/10.1021/es3039104.

Gustin, M.S., Lyman, S.N., Kilner, P., Prestbo, E. (2011) Development of a passive sampler for gaseous mercury. Atmospheric Environment, 45(32), 5805–5812, https://doi.org/10.1016/j.atmosenv.2011.07.014.

Han, Y.-J., Holsen, T.M., Lai, S.O., Hopke, P.K., Yi, S.M., Liu, W., Pagano, J., Falanga, L., illigan, M., Andolina, C. (2004) Atmospheric gaseous mercury concentrations in New York State: relationships with meteorological data and other pollutants. Atmospheric Environment, 38, 6431–6446, https://doi.org/10.1016/j.atmosenv.2004.07.031.

Han, Y.-J., Kim, J.-E., Kim, P.-R., Kim, W.-J., Yi, S.-M., Seo, Y.-S., Kim, S.-H. (2014) General trend of atmospheric mercury concentrations in urban and rural areas in Korea and characteristics of high-concenration events. Atmospheric Environment, 94, 754–764, https://doi.org/10.1016/j.atmosenv.2014.06.002.

Harner, T., Shoeib, M., Diamond, M., Stern, G., Rosenberg, B. (2004) Using passive air samplers to assess urban - Rural trendsfor persistent organic pollutants. 1. Polychlorinated biphenyls and organochlorine pesticides. Environmental Science & Technology, 38, 4474–4483, https://doi.org/10.1021/es040302r.

Horowitz, H.M., Jacob, D.J., Zhang, Y., Dibble, T.S., Slemr, F., Amos, H.M., Schmidt, J.A., Corbitt, E.S., Marais, E.A., Sunderland, E.M. (2017) A new mechanism for atmospheric mercury redox chemistry : implications for the global mercury budget. Atmospheric Chemisty & Physics, 17, 6353–6371, https://doi.org/10.5194/acp-17-6353-2017.

Huang, C., Tong, L., Dai, X., Xiao, H. (2018) Evaluation and application of a passive air sampler for atmospheric volatile organic compounds. Aerosol and Air Quality Research, 18, 3047–3055, https://doi.org/10.4209/aaqr.2018.03.0096.

Huang, J., Choi, H.-D., Landis, M.S., Holsen, T.M. (2012) An application of passive samplers to understand atmospheric mercury concentration and dry deposition spatial distributions. Journal of Environmental Monitoring, 14, 2976–2982, https://doi.org/10.1039/c2em30514c.

Huang, J., Lyman, S.N., Hartman, J.S., Gustin, M.S. (2014) A review of passive sampling systems for ambient air mercury measurements. Environmental Sciences: Processes and Impacts, 16(3), 374–392, https://doi.org/10.1039/c3em00501a.

Hynes, A.J., Donohoue, D.L., Good site, M.E., Hedge cock, I.M. (2009) Our current understanding of major chemical and physical processes affecting mercury dynamics in the atmosphere and at the air-water/terrestrial interfaces. In Mercury Fate and Transport in the Global Atmosphere, Mason, R., Pirrone, N., Eds., Springer: New York, 427–457, https://doi.org/10.1007/978-0-387-93958-2_14.

Jeon, J.-W., Han, Y.-J., Cha, S.-H., Kim, P.-R., Kim, Y.-H., Kim, H., Seok, G.-S., Noh, S. (2019) Application of the Passive Sampler Developed for Atmospheric Mercury and Its Limitation. Atmosphere, 10(11), 678, https://doi.org/10.3390/atmos10110678.

Kim, K., Yoon, H., Brown, R.J., Jeon, E., Sohn, J., Jung, K. (2013) Simultaneous monitoring of total gaseous mercury at four urban monitoring stations in Seoul, Korea. Atmospheric Research, 132, 199–208, https://doi.org/10.1016/j.atmosres.2013.05.023.

Lee, G., Kim, P., Han, Y., Holsen, T.M., Seo, Y., Yi, S. (2016) Atmospheric speciated mercury concentrations on an island between china and korea : Sources and transport pathways. Atmospheric Chemistry and Physics, 16(6), 4119–4133, https://doi.org/10.5194/acp-16-4119-2016.

Lin, C.J., Pehkonen, S.O. (1999) The chemistry of atmospheric mercury: A riview. Atmospheric Environment, 33, 2067–2079, https://doi.org/10.1016/s1352-2310(98)00387-2.

Lyman, S.N., Gustin, M.S., Prestbo, E.M. (2010) A passive sampler for ambient gaseous oxidized mercury concentrations. Atmospheric Environment, 44, 246–252, https://doi.org/10.1016/j.atmosenv.2009.10.008.

Massman, W.J. (1999) Molecular diffusivities of Hg vapor in air, O_2 and N_2 near STP and the kinematic viscosity and thermal diffusivity of air near STP. Atmospheric Environment, 33, 453–457, https://doi.org/10.1016/s1352-2310(98)00204-0.

May, A.A., Ashman, P., Huang, J., Dhaniyala, S., Holson, T.M. (2011) Evaluation of the polyurethane foam (PUF) disk passive air sampler: Computational modeling and experimental measurements. Atmospheric Environment, 45,

4354–4359, https://doi.org/10.1016/j.atmosenv.2011.05.052.

McLagan, D.S., Mazur, M.E.E., Mitchell, C.P.J., Wania, F. (2016a) Passive air sampling of gaseous elemental mercury: a critical review. Atmospheric Chemisty & Physics, 16, 3061–3076, https://doi.org/10.5194/acp-16-3061-2016.

McLagan, D.S., Mitchell, C.P.J., Huang, H., Lei, Y.D., Cole, A.S., Steffen, A., Hung, H., Wania, F. (2016b) A high-precision passive air sampler for gasoues mercury. Environmental Science & Technology, 3, 24–29, https://doi.org/10.1021/acs.estlett.5b00319.

McLagan, D.S., Mitchell, C.P.J., Huang, H., Hussain, B.A., Lei, Y.D., Wania, F. (2017) The effects of meteorological parameters and diffusive barrier reuse on the sampling rate of a passive air sampler for gaseous mercury. Atmospheric Measurement Techniques, 10, 3651–3660, https://doi.org/10.5194/amt-10-3651-2017.

McLagan, D.S., Mitchell, C.P.J., Steffen, A., Hung, H., Shin, C., Stupple, G.W., Wania, F. (2018) Global evaluation and calibration of a passive air sampler for gaseous mercury. Atmospheric Chemistry and Physics, 18(8), 5905–5919, https://doi.org/10.5194/acp-18-5905-2018.

Nishikawa, M., Shiraishi, H., Yanase, R., Tanida, K. (1999) Examination of an improved passive sampler for gaseous mercury on the landfill site. Journal of Environmental Chemistry, 9, 681–684, https://doi.org/10.5985/jec.9.681.

Park, J.-M., Lee, S.-B., Kim, H.-C., Song, D.-J., Kim, M.-S., Kim, M.-J., Kim, Y.-H., Lee, S.-H., Kim, J.-C., Lee, S.-J. (2010) Characteristics of Mercury Emission from Zinc Smelting Facilities. Journal of the Korean Atmospheric Environment, 26(5), 507–516, https://doi.org/10.5572/kosae.2010.26.5.507.

Park, S.-Y., Holsen, T.M., Kim, P.-R., Han, Y.-J. (2014) Laboratory investigation of factors affecting mercury emissions from soils. Environmental Earth Sciences, 7, 2711–2721, https://doi.org/10.1007/s12665-014-3177-x.

Peterson, C., Alishahi, M., Gustin, M.S. (2012) Testing the use of passive sampling systems for understanding air mercury concentrations and dry deposition across Florida, USA. Science of the Total Environment, 424, 297–307, https://doi.org/10.1016/j.scitotenv.2012.02.031.

Poissant, L., Amyot, M., Pilote, M., Lean, D. (2000) Mercury water-air exchange over the upper St. Lawrence river and Lake Ontario. Environmental Science & Technology, 34, 3069–3078, https://doi.org/10.1021/es990719a.

Poissant, L., Pilote, M., Beauvais, C., Constant, P., Zhang, H.H. (2005) A year of continuous measurements of three atmospheric mercury species (GEM, RGM and Hg_p) in southern quebec, canada. Atmospheric Environment, 39(7), 1275–1287, https://doi.org/10.1016/j.atmosenv.2004.11.007.

Pozo, K., Harner, T., Shoeib, M., Urrutia, R., Barra, R., Parra, O., Focardi, S. (2004) Passive-sampler derived air concentrations of persistent organic pollutants on north-south transect in Chile. Environmental Science & Technology, 38, 6529–6537, https://doi.org/10.1021/es049065i.

Schroeder, W.H., Munthe, J. (1998) Atmospheric mercury an overview. Atmospheric Environment, 32(5), 809–822, https://doi.org/10.1016/s1352-2310(97)00293-8.

Scott, J.E., Ottaway, J.M. (1981) Determination of mercury vapour in air using a passive gold wire sampler. Analyst, 106, 1076–1081, https://doi.org/10.1039/an9810601076.

Shoeib, M., Harner, T. (2002a) Using measured octanol-air partition coefficients to explain environmental partitioning of organochlorine pesticides. Environmental Toxicology & Chemistry, 21, 984–990, https://doi.org/10.1002/etc.5620210513.

Shoeib, M., Harner, T. (2002b) Characterization and comparison of three passive air samplers for persistent organic pollutants. Environmental Science & Technology, 36, 4142–4151, https://doi.org /10.1021/es020635t.

Si, L., Ariya, P.A. (2018) Recent advances in atmospheric chemistry of mercury. Atmosphere, 76, 1–18, https://doi.org/10.3390/atmos9020076.

Skov, H., Sorensen, B.T., Landis, M.S., Johnson, M.S., Sacco, P., Goodsite, M.E., Lohse, C., Christiansen, K.S. (2007) Performance of a new diffusive sampler for Hg^0 determination in the troposphere. Environmental Chemistry, 4(2), 75–80, https://doi.org/10.1071/en06082.

Slemr, F., Schuster, G., Seiler, W. (1985) Distribution, speciation, and budget of atmospheric mercury. Journal of Atmospheric Chemistry, 3(4), 407–434, https://doi.org/10.1007/bf00053870.

Stupple, G.W., McLagan, D.S., Steffen, A. (2019) In situ reactive gaseous mercury uptake on radiello diffusive barrier, cation exchange membrane and Teflon filter membrane during atmospheric mercury depletion events. In Proceedings of the 14th International Conference on Mercury as a Global Pollutant, Krakow, Poland, 8–13.

United Nations Environment Programme. (2013) Globla mercury assessment 2013. UNEP. 1–44.

Valente, R.J., Shea, C., Humes, K.L., Tanner, R.L. (2007) Atmospheric mercury in the great smoky mountains compared to regional and global levels. Atmospheric Environment, 41(9), 1861–1873, https://doi.org/10.1016/j.atmosenv.2006.10.054.

Vuong, Q.T., Kim, S.J., Nguyen, T.N.T., Thang, P.Q., Lee, S.J., Ohura, T., Choi, S.D. (2020) Passive air sampling of halogenated polycyclic aromatic hydrocarbons in the largest industrial city in Korea: Spatial distributions and source identification. Journal of Hazardous Materials, 382, 121238, https://doi.org/10.1016/j.jhazmat.2019.121238.

Wan, Q., Feng, X., Lu, J., Zheng, W., Song, X., Han, S. (2009) Atmospheric mercury in changbai mountain area, northeastern china I. the seasonal distribution pattern of total gaseous mercury and its potential sources. Environmental Research, 109(3), 201–206, https://doi.org/10.1016/j.envres.2008.12.001.

Wan, Q., Feng, X., Lu, J., Zheng, W., Song, X., Li, P. (2009) Atmospheric mercury in changbai mountain area, northeastern china II. the distribution of reactive gaseous mercury and particulate me1rcury and mercury deposition fluxes. Environmental Research, 109(6), 721–727, https://doi.org/10.1016/j.envres.2009.05.006.

Wania, F., Shen, L., Lei, Y.D., Teixeira, C., Muir, D.C.G. (2003) Development and calibration of a Resin-based passive sampling system for monitoring persistent organic pollutants in

the atmosphere. Environmental Science & Technology, 37, 1352–1359, https://doi.org/10.1021/es026166c.
Won, J.H., Lee, T.G. (2012) Estimeation of total annual mercury emission from cement manufacturing facilities in Korea. Atmospheric Environment, 62, 265–271, https://doi.org/10.1016/j.atmosenv.2012.08.035.
Zhang, W., Tong, Y., Hu, D., Ou, L., Wang, X. (2012) Characterization of atmospheric mercury concentration along an urban-rural gradient using a newly developed passive sampler. Atmospheric Environment, 47, 26–32, https://doi.org/10.1016/j.atmosenv.2011.11.046.